Infection, Genetics and Evolution 75 (2019) 103971

Contents lists available at ScienceDirect

Infection, Genetics and Evolution

journal homepage: www.elsevier.com/locate/meegid

Research paper

Characterization of previously identified novel DNA fragment associated with Pathogenicity Island III_{536} reveals new *bla*$_{CTX-M}$ gene

Ali Salman Bin Thani*

Department of Biology, College of Science, Bahrain

ARTICLE INFO

Keywords:
Enterobacteriaceae
Extended-spectrum beta-lactamases
Pathogenicity islands
Uropathogenic *Escherichia coli*
Virulence determinants

ABSTRACT

In the Kingdom of Bahrain a high percentage of extra-intestinal infectious diseases are reported as urinary tract infections UTIs. These UTIs are repeatedly diagnosed as multidrug resistant isolates. In a recent investigation, a novel DNA segment was identified in a UTI cefotaxime resistant *Escherichia coli* isolate. The DNA sequence was associated to pathogenicity island III_{536} locus. The current work is investigating/elucidating the genomic context of the newly identified locus in the UTI isolate using Single Genome Specific Primer-PCR (SGSP-PCR) approach. The isolate was characterized and redefined as strain EC1091 (genotype: *bla*$_{TEM}$, *bla*$_{CTX-M}$, *gyrB, chuA*, *yjaA*, TSpE4.C2) and its novel genomic contents were found to acquire antibiotic resistance genes: *bla*$_{CTX-M}$ and *aac (3)*. The *bla*$_{CTX-M}$ was found to be a new beta-lactamase allele with no significant BLASTN results in the National Center for Biotechnology Information (NCBI), but a protein PSI-BLAST against non-redundant database revealed a remote similarity to CTX-M proteins.

1. Introduction

In a previous study a novel DNA sequence was associated with pathogenicity island III_{536} (PAI III_{536}) locus during a screening for virulence determinants (Thani, 2018). The new DNA segment was found in urinary tract pathogenic isolate for a 10 years old female with CTX-M resistance profile. The isolate showed susceptibility to the following antibiotics: ciprofloxacin (MIC ≤0.5), levofloxacin (MIC ≤1), cefuroxime (MIC ≤4), ceftriaxone (MIC ≤1), cefoxitin (MIC ≤4), cefepime (MIC ≤1), gentamicin (MIC ≤2), amikacin (MIC ≤8), piperacillin-tazobactam (MIC ≤4/4), imipenem (MIC ≤1), meropenem (MIC ≤1), ertapenem (MIC ≤0.25), tigecycline (MIC ≤1), trimethoprim-sulfamethoxazole (MIC ≤1/19), nitrofurantoin (MIC ≤16) and one intermediate susceptibility to cephalothin (MIC 16). BLASTN search for the previously identified novel DNA segment did not reveal any similarity hits (Thani, 2018). The sequence was translated and resubmitted to TBLASTX and a reverse open reading frame ORF was found to hit a flagellar motor switch protein FliN/peptidase S58 (Thani, 2018). This protein is involved in bacterial cell movement (Thani, 2018). Therefore, the novel sequence was proposed to play a role in mobility and being part of a fitness island. However, the score (47.8 bits) and the expect (0.012) values of the TBLASTX search require further examination to confirm the obtained results.

In the current work the newly identified DNA sequence found in PAI III_{536} genomic locus is interrogated for new virulence determinants by Single Genome Specific Primer-PCR (SGSP-PCR) (Andrey V. Karlyshev et al., 2000). This method is considered quick genome walking approach to elucidate and investigate novel genomic regions as well as illustrating PAI III_{536} virulence determinants such as S-fimbriae and iron siderophore systems (Leipold et al., 2004; Dobrindt et al., 2002; Monroy-Pérez et al., 2017; Hartsch et al., 2001). The structure of PAI III_{536} is also well known for the presence of many mobile genetic elements such as integrase genes e.g., *intB* as well as insertion sequences e.g., IS*100* (Leipold et al., 2004; Dobrindt et al., 2002; Hartsch et al., 2001). These are involved in the excision of the island from its location downstream of tRNA gene *thrW* (Leipold et al., 2004; Dobrindt et al., 2002; Hartsch et al., 2001). The produced amplicons from SGSP-PCR will be analyzed for sequence similarity in mobile genetic elements MGE databases/tools (e.g., ISfinder, ISsaga, Integrall, ACLAME, tRNAScan, Mobilome-FINDER and PATRIC) (Gourbeyre et al., 2011; Pereira et al., 2009; Lowe and Chan, 2016; Harrison et al., 2007; Siguier et al., 2006; Raphae¨ l Leplae et al., 2010; Wattam et al., 2016). The reason for using these databases/tools is that they provide broader coverage of MGE and they enable *de nevo* predictions and annotations of novel horizontally transferred genes.

* Corresponding author.
E-mail address: abinthani@uob.edu.bh.

https://doi.org/10.1016/j.meegid.2019.103971
Received 27 March 2019; Received in revised form 14 July 2019; Accepted 16 July 2019
Available online 18 July 2019

Table 1
List of the non-contiguous/single reads found in PAI III_{536} locus.

Non-contiguous/single reads	length	Product	Location (nt positions) [a]	UniProt reference clusters ID[b]	Cluster name
EC1091_E00001	308	Aminoglycosiden-acetyltransferase AAC(3)IId	19–240	UniRef100_V0YM76	Aminoglycoside-N(3)-acetyltransferase[c]
EC1091_E00002	597	CTX-M	107–481	UniRef100_A0A159ZLT4	Beta-lactamase[d]
EC1091_E00003	781	Maltodextrin glucosidase	75–293	UniRef50_A0A377AZ29	Maltodextrin glucosidase[es]
EC1091_E00004	617	Misc-feature [f]	Complement (225–542)	UniRef90_A0A3M7UAX6	Uncharacterized protein
EC1091_E00005	234	Misc-feature [f]	57–233	UniRef90_A0A1A8YMW4	Uncharacterized protein
EC1091_E00006	579	Misc-feature [f]	Complement (197–469)	No BLAST Hits available	Not available
EC1091_E00007	631	Misc-feature [f]	64–294	UniRef90_Q8X902	S-ribosylhomocysteine lyase
EC1091_E00008	400	Misc-feature [f]	216–398	UniRef100_A0A1S9ZUH7	Uncharacterized protein
EC1091_E00009	521	Misc-feature [f]	295–519	UniRef90_A0A072PY06	Uncharacterized protein
EC1091_E00010	688	Misc-feature [f]	Complement (47–307)	UniRef100_A0A3B6ZP66	Plasmid replication initiation protein
EC1091_E00011	707	Misc-feature [f]	Complement (379–678)	UniRef90_A0A1B3NIB5	Peroxiredoxin, Ohr subfamily protein
EC1091_E00012	727	Misc-feature [f]	238–618	UniRef90_A0A166GX60	DNase I-like protein
EC1091_E00013	366	Misc-feature [f]	349–621	UniRef90_A0A1J4KEE6	Uncharacterized protein
EC1091_E00014	628	Anion permease [g]	83–271	UniRef100_A0A0D8VFH6	Citrate:succinate antiporter
EC1091_E00015	247	Misc-feature [f]	Complement (3 − 203)	UniRef100_A2XQA6	Uncharacterized protein
EC1091_E00016	238	Misc-feature [f]	2–238	UniRef100_A0A2U2B4Y0	tRNA-specific 2-thiouridylase MnmA
EC1091_E00017	537	Misc-feature [f]	Complement (3–299)	UniRef90_A0A2I4B8C0	uncharacterized protein
EC1091_E00018	444	Misc-feature [f]	Complement (1 − 210), Complement (324–407)	UniRef90_K9CAF8	Uncharacterized protein
EC1091_E00019	267	Misc-feature [f]	Complement (1–267)	UniRef90_A0A1D8ARW6	Uncharacterized protein
EC1091_E00020	288	Misc-feature [f]	43–234	UniRef90_W6EM18	Putative type IIs restriction endonuclease
EC1091_E00021	230	Misc-feature [f]	Complement (2–205)	UniRef100_A0A1M4SVV5	Uncharacterized protein
EC1091_E00022	397	Hypothetical protein	Complement (200–385)	UniRef50_A0A1Q6AD69	Uncharacterized protein

[a] nt = nucleotide.
[b] https://www.uniprot.org/uniref [17].
[c] Accession number (MK421976).
[d] BioProject (PRJNA518024).
[e] Accession number (MK471255).
[f] BLASTN and PSI-BLASTP produced no significant results. The results were also confirmed by MGE databases/tools.
[g] Accession number (MK450313).

2. Materials and methods

2.1. Cultivation conditions

The isolate was grown overnight in Luria-Bertani (LB) broth at 37 °C prior to DNA extraction. DNA extraction was performed according to the manufacturer instructions (MO BIO).

2.2. EC1091 genotyping

EC1091 was characterized by PCR and found to be with the following geneotype: bla_{TEM}, $bla_{CTX\text{-}M\text{-}15}$, *gyrB, chuA*, *yjaA*, TSpE4.C2 (Thani, 2017).

2.3. Single genome specific primer-PCR (SGSP-PCR) and PCR products cleaning

In SGSP-PCR a panel of different restriction enzymes is used to produce genomic restriction digests. These are ligated to their corresponding restriction digests of vector fragments (Andrey V. Karlyshev et al., 2000). In the current study, the following enzymes were used to construct the genomic libraries: (*Eco*RI, *Hin*dIII, *Bam*HI and *Sal*I). The genomic DNA was extracted using UltraClean Microbial DNA isolation kit (MO BIO). The extracted DNA and pBLU (Calorlina) vector were digested with restriction enzymes above, and then were mixed in a ratio of 5:1 genomic DNA to pBLU vector (Andrey V. Karlyshev et al., 2000). After ligation, 1 µl of the genomic library was used in a 25 µl SGSP-PCR reaction. 0.5 units of KAPA2G Fast DNA polymerase and 0.1 µM of forward and reverse primers were used. The primers used in the SGSP-PCR included the two previously used primers to amplify the novel DNA segment sfaAI.1 and sfaAI.2 (Thani, 2018) and four more primers introduced in this study pBLUF: TGCCGGAAACCAGGCAAAGC, pBLUR: AGCGGAAGAGCGCCCAATAC, E112_III_536F: AGGATGACTTGCGTCA CGTT and E112_III_536R: CGGGAGGTGGGTGATGTATG. Primers pBLUF and pBLUR were designed using the sequence for pBLU vector. While, the other two primers (E112_III_536F and R) were designed using the novel DNA sequence. The rationale behind using these primers is to increase the panel of available primers used in the SGSP-PCR reactions. The coordinates for E112_III_536F and R within the novel DNA fragment are (215–234) and (286–305) accordingly.

The SGSP-PCR cycles were as following (TECHNE GENIUS Thermocycler): initial denaturation for 2 min at 95 °C. Then 35 cycles of 10 s denaturation step at 95 °C, 10 s annealing at 55 °C and 5 s extension at 72 °C. A final extension was performed at 72 °C for 10 min. The PCR products were cleaned using MO BIO kits and then sent for sequencing (Macrogen Inc., Seoul).

2.4. RNA extraction and reverse transcription PCR

The total RNA extraction was done following the protocol from the manufacturer (MO BIO kit). For the reverse transcriptase PCR, 5 µl of the extracted RNA was used in a 50 µl MasterMix reaction (AccessQuick RT-PCR System from Promega) with 5 units of AMV reverse transcriptase. The PCR conditions were as following (TECHNE GENIUS Thermocycler): a reverse transcription step for 45 min at 45 °C and then initial denaturation for 2 min at 95 °C. Then 35 cycles of 15 s denaturation step at 95 °C, 15 s annealing (temperatures varied upon different primers used) and 3 s extension at 72 °C. A final extension was performed at 72 °C for 10 min.

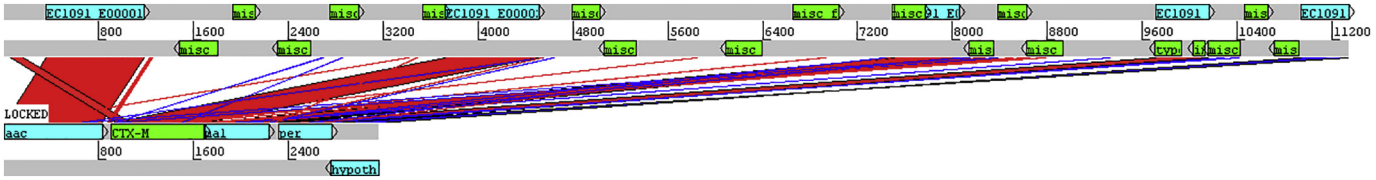

Fig. 1. Schematic representation of the gene cassette for the PAI III_{536} locus. The pairwise comparison is between the gene cassette for PAI III_{536} locus and their correspondent subject genes by BLASTN homology search. The red and blue colors between the compared DNA lines indicate the presence of matches or inversions, respectively. The schematic was produced using ACT program (https://www.sanger.ac.uk/science/tools/artemis-comparison-tool-act). (For interpretation of the references to colour in this figure legend, the reader is referred to the web version of this article.)

2.5. Sequence analysis, formation of non-contiguous DNA fragments, annotation, and accession numbers

PCR products were sequenced using Sanger Technology (Macrogen Inc., Seoul). Amplicons' sequence assembly and formation of non-contiguous DNA fragments were performed using Clone Manager (version 9). The Use of SGSP-PCR approach produced a total number of 37 amplicons. These were screened for vector contamination using the National Centre for Biotechnology Information (NCBI) VecScreen tool. Eleven were either vector contaminated or too short, and were excluded from further analysis. The remaining 26 (11,337 bases) amplicons were used in de novo assembly. The following running parameters were used in Clone Manager: expected coverage 6× and overlap score of 50 with sequence shuffle. Two contiguous fragments were produced and were confirmed using BLASTN homology search. Both were produced using three sequence reads. The remaining sequences (20) were regarded as single ends. These were analyzed and searched for homology in different MGE databases/tools. The results of this analysis are present in (Table 1). The sequences were deposited in NCBI as either raw data (NCBI BioProject PRJNA518024) or to GenBank (accession numbers: MK421976, MK450313 and MK471255). The sequences are also provided in the supplementary materials. The results indicated the presence of non-contiguous DNA fragments with 17 (this number comes after joining 6 single ends in two contiguous fragments and then subtracting the joined reads (4) from the original 21 contigs) showing no significant similarity in NCBI databases.

2.6. Alignment of EC1091_E00002 against other CTX-M proteins and construction of the phylogenetic tree

The ORF for EC1091_E00002 obtained by ORFFinder (NCBI) was used in BLASTP homology search (Table 1). The amino acid sequence for 32 homologous proteins were aligned with the amino acid sequence for the ORF of EC1091_E00002 using ClustalW (version 1.83) (Larkin et al., 2007). The multiple alignment file was used to construct phylogenetic tree by neighbor from PHYLIP 3.695 (Felsenstein, 1989). The tree was illustrated using TreeView (D.M.Page, R, 1996).

3. Results and discussion

3.1. The Gene cassette structure for the PAI III_{536} locus in EC1091

Uropathogenic *Escherichia coli* (UPEC) possesses several virulence factors that enable the microbe to cause serious urinary tract infections (UTIs). Among Uropathogenic strains, *E. coli* 536 has many of these virulence determinants distributed between its pathogenicity islands (PAI I_{536} to V_{536}). This include the α-hemolysin gene clusters, the salmochelin and yersiniabactin siderophore systems and different types of fimbrial adhsins (Dobrindt et al., 2002; Hartsch et al., 2001). Fimbrial adhsins play specific role in mediating the transition of infection from acute to chronic diseases (Leipold et al., 2004; Dobrindt et al., 2002; Hartsch et al., 2001). This is because during the infection the pathogen might change the expression of certain adhsins upon the type of tissue they colonize (Leipold et al., 2004; Dobrindt et al., 2002; Hartsch et al., 2001). In PAI III_{536} sfa_I encoding the S-family adhesins recognize the α-sialyl-2-3-β-lactose-containing receptors (Hartsch et al., 2001). The expression of this adhesin contributed to the infection development in sepsis, meningitis and UTI strains (Hartsch et al., 2001). Furthermore, the structure of PAI III_{536} is unstable due to the presence of many mobile genetic elements such as the *int*-bacteriophage SfX like integrase gene (Dobrindt et al., 2002; Hartsch et al., 2001).

When compared to strain 536, *E. coli* EC1091 showed positive results for two pathogenicity islands' markers (PAI III_{536} and PAI IV_{536}). As illustrated by previous screening studies, the determinants for PAI IV_{536} were detected in different *E. coli* pathovars and the island was less subject to genetic variation and excision processes exhibited by the other four PAIs of strain 536 (Leipold et al., 2004). The PCR detection of PAI IV_{536} determinant in EC1091 indicates the presence of the siderophore system, which is important for the survival of the pathogen inside the host (Leipold et al., 2004). On the other hand, the structure of PAI III_{536} is characterized by the S-family adhesins (Hartsch et al., 2001). However, the current investigation illustrated that none of the CDS obtained for the novel locus is related to the fimbrial adhsins (Table 1).

In this study, the structure of the gene cassette was analyzed by different NCBI and other MGE databases/tools (Table 1, "product"). However, another BLAST search by UniProt (https://www.uniprot.org/uniref) revealed more functions added to the mosaic structure of the locus. In general many plasmid related proteins were elucidated e.g., the antibiotic resistance proteins and the plasmid replication initiation protein (Fig. 1 and Table 1). Thus, the preliminary investigation carried in this study by the SGSP-PCR proved the mosaic structure of the locus with possible suggestion for a plasmid origin of the acquired genes. Nevertheless, other possible origins for the locus cannot be excluded (e.g., bacteriophages or Pathogenicity Islands). Therefore, there is a need for a whole genome sequencing to illustrate the full structure of the DNA segment. One CDS (EC1091_E00007) referred to S-ribosylhomocysteine lyase is involved in the synthesis of quorum sensing protein autoinducer 2 (AI-2), which regulates important traits and adaptive physiological processes (Zeng and Lin, 2013). Different studies indicated that the deletion of the this gene would render the avian pathogenic *E. coli* strains avirulent (Han et al., 2013). Other sequences in the locus were not identified and were regarded as uncharacterized or hypothetical proteins.

3.2. Antibiotic resistance genes

The identified antibiotic resistance genes were (EC1091_E00001) *aac (3)* encoding aminoglycoside *N*-acetyltransferase and (EC1091_E00002) $bla_{CTX\text{-}M}$ (extended-spectrum beta-lactamase). The *aac (3)* sequence was deposited to GenBank under the accession number (MK421976) as partial CDS. The $bla_{CTX\text{-}M}$ sequence was deposited as raw nucleotide sequence under BioProject PRJNA518024. The aminoglycoside *N*-acetyltransferase AAC(3) IId allele is involved in the modification of aminoglycoside antibiotics by using the acetyl-coenzyme A as a donor (Dell'Amico et al., 2003; Levings et al., 2005; Shakil et al., 2008; Da Qi et al., 2017). This affects the functions of the amino group and thus confers resistance to the following antibiotics:

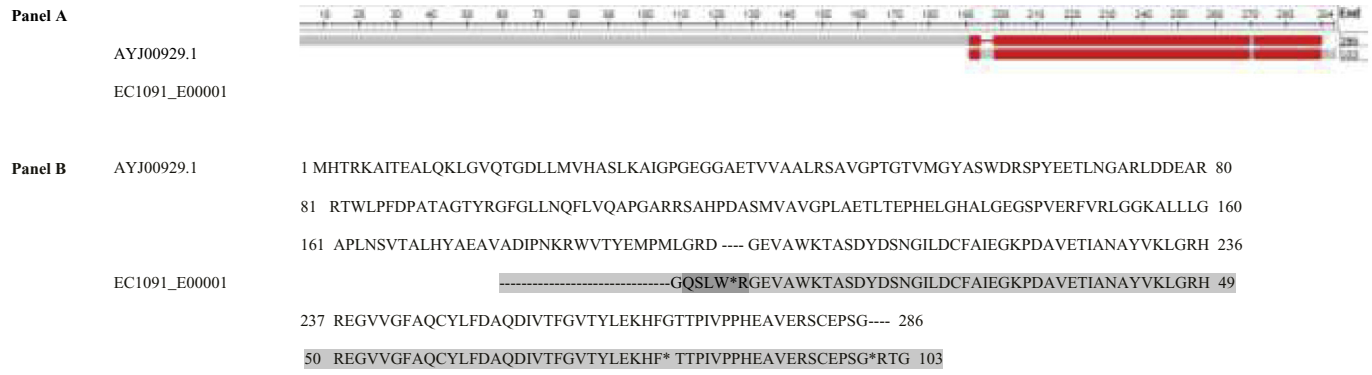

Fig. 2. Panel A. Graphical overview for the Constraint-based Multiple Alignment Tool (COBALT) from NCBI. The amino acid sequence for the protein AYJ00929.1 (aminoglycoside N-acetyltransferase AAC(3)-IId in *Escherichia coli*) is aligned to the sequence for EC1091_E00001 (BLASTP Expect of $1^{e\text{-}54}$, ID 100%, Gaps 0). The shaded grey box refers to the insertion in the EC1091_E00001 sequence (amino acids 193 to 198). **Panel B.** Sequence alignment showing the 103 amino acids for EC1091_E00001 shaded in light grey and the insertion sequence in dark grey box. * refers to stop codons.

gentamicin, sisomicin, and fortimicin but not tobramycin, amikacin, and kanamycin (Dell'Amico et al., 2003; Levings et al., 2005; Shakil et al., 2008). However, in the case of EC1091, the *aac (3)* gene did not produce activity against gentamicin (data are not shown). When investigated, the sequence for EC1091_E00001 indicated the presence of an insertion at amino acids 193 to 198 with stop codon (Fig. 2). The insertion was searched in the Integron Database INTEGRALL (http://integrall.bio.ua.pt/?acc=AF188331) and similarity was found against the sequence of TnSF1 (accession number AF188331). The presence of this insertion with stop codon explains the susceptibly of strain EC1091 to the minimal inhibitor concentration (MIC) of gentamicin. Therefore, the insertion rendered *aac (3)* gene cryptic.

In a previous study the BLASTN search for the identified novel DNA fragment did not reveal any similarity hits (Thani, 2018). The sequence was translated and resubmitted to TBLASTX and a reverse open reading frame was found to hit a flagellar motor switch protein FliN/peptidase S58 (Thani, 2018). This protein is involved in bacterial cell movement (Thani, 2018). Therefore, the novel sequence was proposed to play a role in mobility and being part of a fitness island. However, the score (47.8 bits) and the expect (0.012) values for the TBLASTX search previously obtained require further examination to confirm the results obtained. In this study, the amino acid sequence for the novel DNA fragment is rechecked and was identified as new $bla_{\text{CTX-M}}$ gene (Figs. 3 and 4). ORFFinder from NCBI (https://www.ncbi.nlm.nih.gov/orffinder/) was used to produce possible ORFs. These were used in BLASTP search using the following running settings and algorithms (database: non-redundant protein sequences (nr), and Position-specific iterated PSI-BLAST). The PSI-BLAST is used to detect distantly related proteins (Jones and Swindells, 2002). This is facilitated by the position-specific scoring matrix (PSSM), which searches the database using protein–protein BLAST for new matches (Jones and Swindells, 2002). The $bla_{CTX\text{-}M}$ gene showed differences in its amino acid sequences against other cefotaxime resistance genes (Figs. 3 and 4). The BLASTP results against one of the subject CTX-M proteins (accession number WP_063860035) produced the following values: score (52.8 bits) and expect ($2e^{-05}$) (Fig. 3). Compared to the previous TBLASTX results the new better PSI-BLAST scores support the proposed function for the novel DNA sequence as a new $bla_{CTX\text{-}M}$ gene. A Neighbor-Joining phylogenetic tree was also constructed using different CTX-M protein sequences (Fig. 4). The tree used the BLASTP results for CTX-M proteins showing similarity to the amino acid sequence for the newly identified $bla_{\text{CTX-M}}$ gene. The tree showed a significant and remarkable uniqueness of the translated amino acid sequence compared to other CTX-M proteins confirming its novel sequence. One distantly related beta-lactamase protein refereed to CTX-M-32 (AFI26317.1) formed a sub-clade with the novel CTX-M. If confirmed by expression studies the newly identified $bla_{\text{CTX-M}}$ would be an interesting entry to the repository of the $bla_{\text{CTX-M}}$ genes. This is because any new information in regards to the antibiotic resistance process would enable a better understanding for the different mechanisms applied by the microbes to modulate their genetic makeup and maintain their extended spectrum beta-lactamases patterns.

class A extended-spectrum beta-lactamase CTX-M-181 [Escherichia coli] Alignment statistic

Score	Expect	Method	Identities	Positives
52.8 bits(125)	$2e^{-05}$	Compositional matrix adjust.	41/114(36%)	53/114(46%)

Query 2 QQQVGGAMTLPDLLAAAALHYNDHATKNKLIPFVARMTCVTLPARPANTPSLP-PRPYPP 60
++ V G M+L +L + AAAL Y +DH NKLI +V VT AR + R P
Sbjct 113 EKHVNGTMSLAEL-SAAALQYSDHVAMNKLIAHVGGPASVTAFARQLGDETFRLDRTEPT 171

Query 61 IHHPPPGHPMLLHTPSPHGTHLTLPNLSLGIRLTPQRSICYVDMWKSFSFPAAS 114
++ PG P T SP T L NL+LG L + V K + AAS
Sbjct 172 LNTAIPGDPR--DTTSPRAMAQTLRNLTLGKALGDSQRAQLVTWMKGNTTGAAS 223

Fig. 3. BLASTP results for the query (ORF translation of EC1091_E00002) against the subject protein for CTX-M (accession number: WP_063860035).

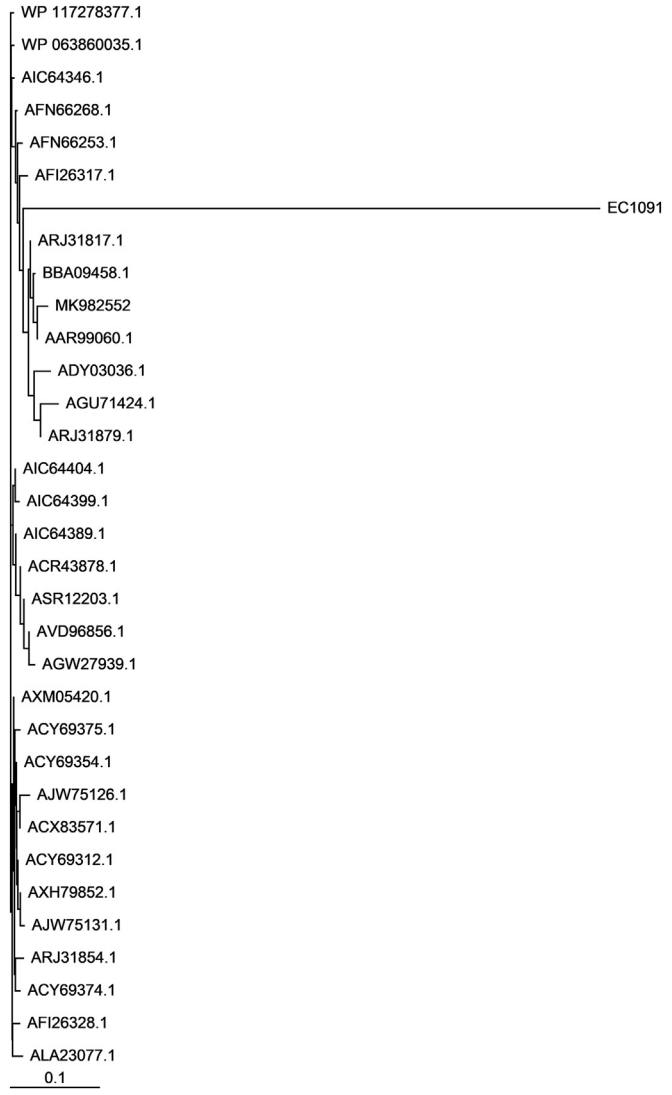

Fig. 4. Phylogenetic tree of CTX-M proteins. The evolutionary history was inferred using the Neighbor-Joining method. The tree is drawn to scale.

3.3. Reverse transcription of the beta-lactamases genes in EC1091 and evolution of the novel $bla_{CTX\text{-}M}$ gene

As mentioned above the reverse transcription of the new identified $bla_{CTX\text{-}M}$ gene would help in understanding the mechanisms applied by different microorganisms to regulate the expression of the beta-lactamase enzymes and their evolution. In this part, a reverse transcription reaction was carried for the virulence determinants (PAI II_{CFT073}, the novel DNA fragment associated with PAI III_{536} and PAI IV_{536}) and the beta-lactamase genes (bla_{TEM}, $bla_{CTX\text{-}M\text{-}15}$) for strain EC1091 (Fig. 5). The reverse transcription PCR was performed before and after antibiotic induction with cefotaxime at a concentration of 1 μg/ml. The results showed a constitutive expression of the following determinants before and after cefotaxime induction: PAI II_{CFT073} and PAI IV_{536} and the beta-lactamase genes (bla_{TEM}, $bla_{CTX\text{-}M\text{-}15}$). The constitutive induction of the beta-lactamases was previously shown to be under the regulation of the peptidoglycan-recycling route (Bagge et al., 2002; Zeng and Lin, 2013). The process involves the release of the muropeptides, which is transported to the cytoplasm by the transmembrane permease proteins (Bagge et al., 2002; Zeng and Lin, 2013). In the cytoplasm, anhydromuropeptides modulate the regulatory activity of the beta-lactamases and upregulate the expression of the *bla* genes (Bagge et al., 2002; Zeng and Lin, 2013). To the contrary, no expression was noted for

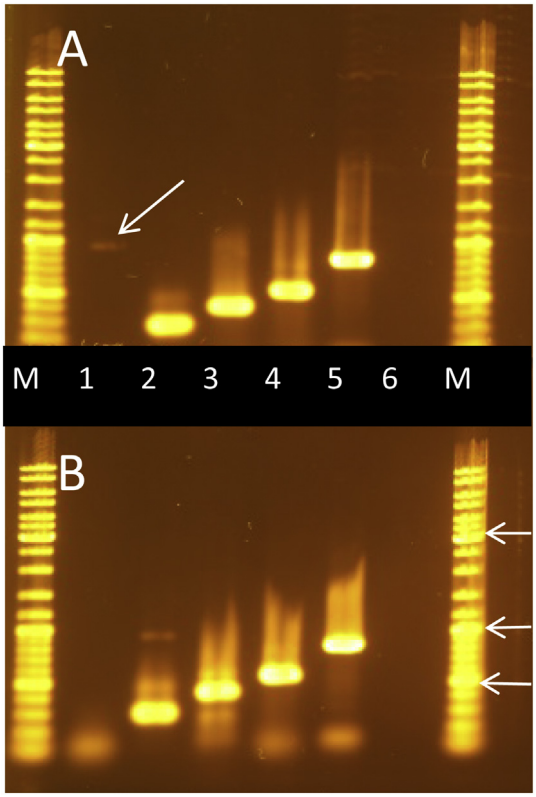

Fig. 5. Reverse transcription PCR for the virulence determinants and beta-lactamase genes in EC1091. 1; PAI III_{536}, 2; PAI IV_{536}, 3; PAI II_{CFT073}, 4; $bla_{CTX\text{-}M\text{-}15}$, 5; bla_{TEM}, 6; negative control and M; GeneRuler DNA marker (ThermoScientific). Panel A refers to RT-PCR under no antibiotic induction. Panel B refers RT-PCR after cefotaxime (1 μg/ml) induction. Arrows next the marker refers to the DNA bands (0.5, 1 and 1.5 kb). Arrow next to the band in panel A refers to the product of PAI III_{536}.

the PAI III_{536} associated novel DNA fragment after cefotaxime induction. However, weak band was observed for the newly identified $bla_{CTX\text{-}M}$ gene in the absence of antibiotic induction (Fig. 5). This indicates that the newly identified *bla* gene is coding for mRNA transcript. Therefore, the newly identified $bla_{CTX\text{-}M}$ gene/the PAI III_{536} associated novel DNA fragment is not a cryptic gene and probably encodes for a protein/function. The DNA for the newly identified $bla_{CTX\text{-}M}$ was translated and used in a BLASTP search against the $bla_{CTX\text{-}M\text{-}15}$ (MK982552) found in EC1091. A high similarity between the two sequences was found (Fig. 6). This could indicate the origin and evolution of the new $bla_{CTX\text{-}M}$ gene. One possible origin for the newly identified $bla_{CTX\text{-}M}$ gene would be a $bla_{CTX\text{-}M\text{-}15}$ gene duplication and DNA recombination.

4. Conclusions

In this study a preliminary investigation for the locus of PAI III_{536} in EC1091 using the SGSP-PCR approach proved the mosaic structure for the locus with indication for a possible plasmid origin of the obtained genes. However, other possible origins for the locus cannot be excluded e.g., bacteriophages or Pathogenicity Islands as these could also harbor mosaic DNA structures with certain episomal moieties. The investigation has also re-annotated the previously novel DNA fragment to be a new $bla_{CTX\text{-}M}$ gene. Further analysis is required to elucidate the virulence and mobile genetic elements in EC1091 by designing primers for the uncharacterized CDS in the novel DNA segment and perform reverse transcription studies to check for gene expression and protein synthesis. This would necessities full genome sequencing for the strain EC1091 and expression study for the new $bla_{CTX\text{-}M}$ gene identified. The current study pinpoints the evolutionary aspects applied by antibiotic

```
NW Score     Identities   Positives    Gaps
52           43/166(26%)  59/166(35%)  45/166(27%)
Query  1     MQ----------------------QQVGGAMTLPDLLAAAALHYNDHATKNKLIPFVAR  37
             M+                      + V G M+L +L +AAAL Y+D+   NKLI  V
Sbjct  1     MEPNLLNQRVEIKKSDLVNYNPIAEKHVNGTMSLAEL-SAAALQYSDNVAMNKLIAHVGG  59
Query  38    MTCVTLPARPANTPSLP-PRPYPPIHHPPPGHPMLLHTPSPHGTHLTLPNLSLGIRLTPQ  96
                VT  AR     +    R  P ++   PG P    T SP     TL NL+LG  L
Sbjct  60    PASVTAFARQLGDETFRLDRTEPTLNTAIPGDPR--DTTSPRAMAQTLRNLTLGKALGDS  117
Query  97    RSICYVDMWKSFSFPAASALVSVSA------------FG------E  124
             +    V   K  +  AAS    + A             +G      +
Sbjct  118   QRAQLVTWMKGNTTGAASIQAGLPASWVVGDKTGSGGYGTQTKNIQ  163
```

Fig. 6. BLASTP results for the query (ORF translation of EC1091_E00002) against the subject protein for CTX-M-15 in EC1091 (accession number: MK982552).

resistance isolate in local hospital. The investigation open new prospective for future studies relating MIC information obtained and the evolution of antibiotic resistance isolates in hospital environment.

Funding

This study was financially supported by a research fund from the Dean of Scientific Research, University of Bahrain (project no. 2011/20).

Declaration of Competing Interest

None.

Appendix A. Supplementary data

Supplementary data to this article can be found online at https://doi.org/10.1016/j.meegid.2019.103971.

References

Bagge, N., Ciofu, O., Hentzer, M., Campbell, J.I.A., Givskov, M., Høiby, N., 2002. Constitutive high expression of chromosomal -lactamase in Pseudomonas aeruginosa caused by a new insertion sequence (IS1669) located in ampD. Antimicrob. Agents Chemother. 46, 3406–3411.

D.M.Page, R, 1996. TreeView: an application to display phylogenetic trees on personal computers. CABIOS Appl. NOTE 12, 357–358.

Da Qi, Zhenbo Xu, Yang, Ling, Li, Bing, Li, Lin, Li, Xiaoxi, Dingqiang Chen, X.X., 2017. Effect of aminoglycosides on the pathogenic characteristics of microbiology. Microb. Pathog. 113, 357–364.

Dell'Amico, M.L.R.E., Luzzaro, F., Amicosante, G., Gian Maria Rossolini, J.-D.D., 2003. Novel 3-N-aminoglycoside Acetyltransferase gene, aac(3)-Ic, from a Pseudomonas aeruginosa Integron. Antimicrob. Agents Chemother. 47, 1746–1748.

Dobrindt, U., Nagy, G., Schneider, G., Johann, A., Gottschalk, G., Blum-Oehler, G., 2002. Genetic structure and distribution of four pathogenicity islands (PAI I(536) to PAI IV (536)) of uropathogenic *Escherichia coli* strain 536. Infect Immun 70, 6365–6372. https://doi.org/10.1128/IAI.70.11.6365-6372. (2002).

Felsenstein, J., 1989. PHYLIP - phylogeny inference package. Cladistics 5, 164–166.

Gourbeyre, A.M.V.E., Charneau, V., Mick Chandler, P.S., 2011. ISsaga is an ensemble of web-based methods for high throughput identification and semiautomatic annotation of insertion sequences in prokaryotic genomes. Genome Biol. 12.

Han, X., Bai, H., Liu, L., Dong, H., Liu, R., Song, J., Ding, C., Qi, K., Liu, H., Yu, S., 2013. The luxS gene functions in the pathogenesis of avian pathogenicEscherichia coli. Microb. Pathog. 55, 21–27.

Harrison, H.-Y.O.E.M., Kulasekara, B.R., Thani, A.B., Kadioglu, A., Lory, S., Hinton, J.C.D., Barer, M.R., Deng, Z., Kumar Rajakumar, X.H., 2007. MobilomeFINDER: web-based tools for in silico and experimental discovery of bacterial genomic islands. Nucleic Acids Res. 35, W97–W104.

Hartsch, U.D.T., Gottschalk, G., Blum-Oehler, G., Ron, E.Z., Jorg Hacker, R.F., 2001. S-Fimbria-encoding determinant sfa(I) is located on pathogenicity island III(536) of uropathogenic Escherichia coli strain 536. Infect. Immun. 69, 4248–4256.

Jones, D.T., Swindells, M.B., 2002. Getting the most from PSI–BLAST. Trends Biochem. Sci. 27, 161–164.

Karlyshev, A.V., Pallen, M.J., Wren, B.W., 2000. Single-primer PCR procedure for rapid identification of transposon insertion sites. Benchmarks 28, 1078–1082.

Larkin, M.A., Blackshields, G., Brown, N.P., Chenna, R., McGettigan, P.A., McWilliam, H., Valentin, F., Wallace, I.M., Wilm, A., Lopez, R., Thompson, J.D., Gibson, T.J., Higgins, D.G., 2007. Clustal W and Clustal X version 2.0. Bioinformatics 23, 2947–2948.

Leipold, Barbara Middendorf Kristina, Dobrindt, Ulrich, Blum-Oehler, Gabriele, Jörg Hacker, B.H., 2004. Instability of pathogenicity islands in Uropathogenic Escherichia coli 536. J. Bacteriol. 186, 3086–3096.

Leplae, Raphae¨ l, Lima-Mendez, Gipsi, Toussaint, Ariane, 2010. ACLAME: a CLAssification of Mobile genetic Elements, update 2010. Nucleic Acids Res. 38, D57–D61.

Levings, Renee S., Partridge, Sally R., Lightfoot, Diane, Hall, Ruth M., Djordjevic, Steven P., 2005. New Integron-associated gene cassette encoding a 3-N-aminoglycoside acetyltransferase. Antimicrob. Agents Chemother. 49, 1238–1241.

Lowe, T.M., Chan, P.P., 2016. tRNAscan-SE on-line: integrating search and context for analysis of transfer RNA genes. Nucleic Acids Res. 44, W54–W57.

Monroy-Pérez, Gloria Luz Paniagua-Contreras Eric, Vaca-Paniagua, Felipe, Díaz-Velásquez, Clara, Uribe-García, Alina, Sergio Vaca, T.-J., 2017. Comprehensive expression analysis of pathogenicity genes in uropathogenic Escherichia coli strains. Microb. Pathog. 103 (1–7).

Pereira, Alexandra Moura Carolina, Leitão, Nuno, Henriques, Isabel, António Correia, M.S., 2009. INTEGRALL: a database and search engine for integrons, integrases and gene cassettes. Bioinformatics 25, 1096–1098.

Shakil, Shazi, Khan, Rosina, Zarrilli, Raffaele, Khan, Asad U., 2008. Aminoglycosides versus bacteria–a description of the action, resistance mechanism, and nosocomial battleground. J. Biomed. Sci. 15, 5–14.

Siguier, P., Perochon, J., Lestrade, L., Mahillon, J., Chandler, M., 2006. ISfinder: the reference centre for bacterial insertion sequences. Nucleic Acids Res. 34, D32–D36.

Thani, A. Bin, 2017. Detection of novel GyrB mutations associated with Escherichia coli clinical isolates. JBBBE 35, 88–95. https://doi.org/10.4028/www.scientific.net/JBBBE.35.88.

Thani, A. Bin, 2018. Identification of novel DNA sequence associated with pathogenicity island III536 locus in Uropathogenic Escherichia coli isolate and distribution of virulence determinants in β-lactam resistant isolates. Microb. Pathog. 123, 393–397.

Wattam, A.R., Davis, J.J., Assaf, R., Boisvert, S., Brettin, T., Bun, C., Conrad, N., Dietrich, E.M., Disz, T., Gabbard, J.L., Gerdes, S., Henry, C.S., Kenyon, R.W., Machi, D., Mao, C., Nordberg, E.K., Olsen, G.J., Murphy-Olson, D.E., Olson, R., Overbeek, R., Parrello, B., Pusch, G.D., Shukla, M., Vonstein, V., Warren, A., Xia, F., Yoo, H., Stevens, R.L., 2016. Improvements to PATRIC, the all-bacterial bioinformatics database and analysis resource Center. Nucleic Acids Res. 45, D535–D542.

Zeng, X., Lin, J., 2013. Beta-lactamase induction and cell wall metabolism in gram-negative bacteria. Front. Microbiol. 4, 1–9.